

TOWARDS BEAMFORMING FOR UWB SIGNALS

Sigmar Ries¹ and Thomas Kaiser²

1: Fachhochschule Südwestfalen
Dept. Meschede
Lindenstr. 53, D-59872 Meschede
Germany
email: ries@fh-swf.de

2: Duisburg-Essen University
Faculty of Engineering
Department of Communication Systems
Bismarckstraße 81, 47048 Duisburg, Germany
email: thomas.kaiser@uni-duisburg.de

ABSTRACT

Beamforming for UWB signals has some special properties that are different from the narrowband case. The investigation of ideal time-delay beamforming for short pulses shows a striking feature, namely the absence of grating lobes in the beampattern. This means that the spacing of the array elements is not limited by half of the wavelength, hence high resolution can be achieved with only a few array elements. Further, the beampatterns sidelobe structure is mainly dependent on the impulse shape. Concerning digital beamforming, a realistic assumption is that only filters with a few coefficients can be used, due to the very high sampling rate needed for digital processing of UWB signals. But again, the use of broadband pulses allows to obtain acceptable digital beampatterns with low complexity. This means that a realization of digital beamforming for UWB signals might be possible in the near future.

1. INTRODUCTION

Ultra-Wideband (UWB) communication systems and Multi-Antenna (MA) systems belong to the few emerging key technologies in wireless communications. In order to avoid strong interference of conventional narrowband transmission systems by ultra-wideband signals, the transmit power of UWB systems is fairly limited, which leads to a restricted coverage. This very weakness is opposite to one of the main strengths of MA techniques; they are able to increase the range. Such a reversal should indicate the potential of a marriage of these two complementary techniques [5].

Numerous others benefits can be envisaged. For example, the capability of Multi-Antenna systems to spatially distinguish among wavefronts impinging from different directions not only facilitate the equalizer design of UWB systems by reduction of delay spread, but rather also enables a further increase in data rate - 1 Gbit/s over air becomes feasible. Moreover, by MA techniques, narrowband and broadband interferers may be almost perfectly suppressed so that the number of concurrent users can be significantly increased [4]. Last but not least a distinct reduction of electromagnetic radiation can be expected from UWB & MA, which in turn may also save battery life.

However, a large number of different challenges do resist. For example, at a first glance digital beamforming seems to be prevented due to the extremely high sampling rate. In contrast, analog beamforming requires

adjustable true time delays, such delays exhibit noticeable tolerance and therefore less precision. The aim of this contribution is to demonstrate some first steps towards beamforming for UWB systems.

2. BEAMFORMING FOR WIDEBAND PULSES

To start with, we consider the case of a linear equispaced array, consisting of N equidistant omnidirectional sensors. If c is the propagation speed, Φ the angle of incidence of an impulse signal $s(t)$ measured with respect to broad-side direction and d the distance between two sensors, then the signal recorded at the n -th sensor is given by

$$s_n(t) = s(t + n \frac{d}{c} \sin(\Phi)), \quad n = 1(1)N. \quad (1)$$

Note that in this preliminary investigation we omit the influence of a real UWB channel, e.g. the multipath propagation.

The ideal "delay and sum" beamformer produces

$$b(\Phi, \Theta, t) = \sum_{n=0}^{N-1} s_n(t - n\tau_{\Theta,n}) \quad (2)$$

where $\tau_{\Theta,n} = (d/c) \sin(\Theta)$ are the *steering delays* and Θ the *steering angle*. In order to achieve a *time-independent* beampattern¹ the total energy of the beamformer output is often used

$$BP(\Theta, \Phi) = \left(\int_{-\infty}^{\infty} |b(\Phi, \Theta, t)|^2 dt \right)^{1/2} \quad (3)$$

which reduces to the conventional narrowband beampattern if $s(t)$ is of sinusoidal type.

We will show now some simulation results for typical UWB signals, as the twice differentiated Gaussian impulse

$$g(t) = (1 - 16\pi(t/\Delta T)^2)e^{-8\pi(t/\Delta T)^2} \quad (4)$$

where the nominal duration ΔT is set to $2 * 10^{-10}$ s, leading to a -3 dB bandwidth from 5 GHz to 11.5 GHz, and an alternate UWB waveform [3]

$$g_\alpha(t) = \frac{1}{1 - \alpha} (e^{-4\pi(t/\Delta T)^2} - \alpha e^{-4\pi(\alpha t/\Delta T)^2}) \quad (5)$$

¹A very similar looking alternative beampattern is defined as [6] $BP(\Theta, \Phi) = \max_t |b(\Phi, \Theta, t)|$

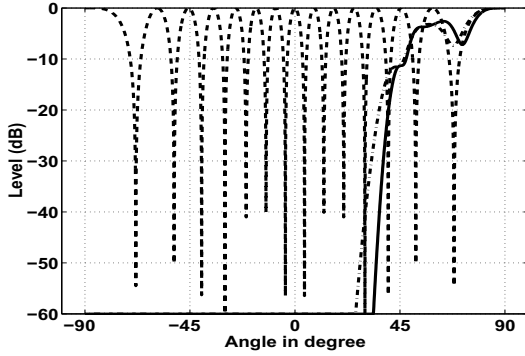


Figure 1: Beam pattern of $g(t)$ (solid line) and $g_\alpha(t)$ (dash-dotted line) impulses arriving at 90° on array 1 with 2 elements at distance $14\lambda/2$ and of narrowband signal with wavelength λ (dashed line)

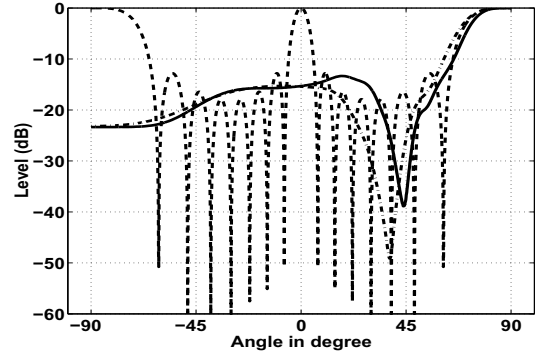


Figure 3: Beam pattern of $g(t)$ (solid line) and $g_\alpha(t)$ (dash-dotted line) impulses arriving at 90° on array 2 with 8 elements at distance λ and of narrowband signal with wavelength λ (dashed line)

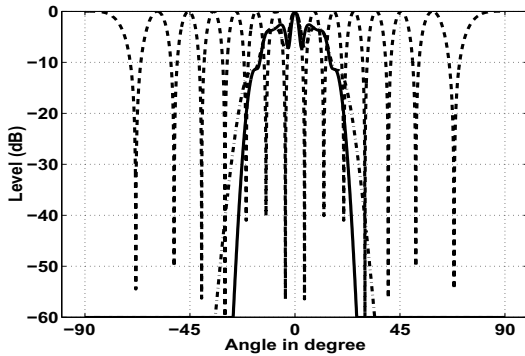


Figure 2: Beam pattern of $g(t)$ (solid line) and $g_\alpha(t)$ (dash-dotted line) impulses arriving at 0° on array 1 with 2 elements at distance $14\lambda/2$ and of narrowband signal with wavelength λ (dashed line)

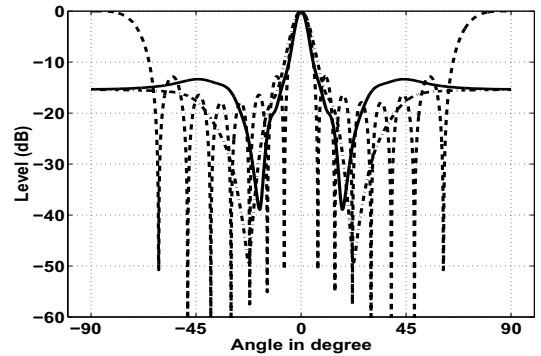


Figure 4: Beam pattern of $g(t)$ (solid line) and $g_\alpha(t)$ (dash-dotted line) impulses arriving at 0° on array 2 with 8 elements at distance λ and of narrowband signal with wavelength λ (dashed line)

where the nominal duration ΔT is set to 2.5×10^{-10} s and the scaling parameter α to 1.5, leading to a -3 dB bandwidth from 3.4 GHz to 8 GHz. The wavelength of the corresponding sinewave is chosen according to a nominal center frequency of 6.85 GHz. Two typical array configurations are considered throughout this paper:

- Array 1 has 2 elements at distance $14\lambda/2$
- Array 2 has 8 elements at distance λ

Hence in the narrowband case, grating lobes will appear in the beam pattern. In the figures, simulated $BP(\Theta, \Phi)$ are shown for signals arriving at 0° and 90° , respectively, and the beam pattern corresponding to $g(t)$, $g_\alpha(t)$ and a sinewave of frequency 6.85 GHz are plotted in the same figure for comparison.

Now, in Figures 1 to 4 a striking feature of impulse beamforming is observed, namely the absence of grating lobes [3, 6]. A simple explanation of this phenomenon is that the grating lobes occur at different angles for different signal frequencies in contrast to the main lobe which is always located at the same angle. Hence, for a broadband signal the grating lobes are averaged out.

Of course, this property is of great importance for UWB array design, since it allows to choose the sensor

distance without the $\lambda/2$ limitation, enabling to achieve high resolution with only a few array elements.

A further interesting property that can be observed in Figures 1 to 4 is the dependence of the beam pattern and especially its sidelobes on the pulse shape. This is the object of further research and may have influence on the pulse shaping in future UWB systems.

3. DIGITAL BEAMFORMING

Consider the sampled outputs $s_n[k]$ of the received analog signals with sampling frequency f_s , then a time delay error $\Delta_{\Theta,n} = \tau_{\Theta,n} f_s - \text{floor}(\tau_{\Theta,n} f_s)$, where $\text{floor}(x)$ means the integer part of x , between the ideal steering delay measured in samples and its preceding sample point will occur. Therefore, some way must be found to recover the desired signal value from its sampled values around $\text{floor}(\tau_{\Theta,n} f_s)$. For this purpose, all digital beamformers use some kind of interpolation [7, 9]. The simplest method is to use nearest-neighbour interpolation (NN-interpolation), thus replacing the signal value at the desired steering delay with the signal value at the nearest sampling point. For narrowband beamforming, nearest-neighbour interpolation is known to pro-

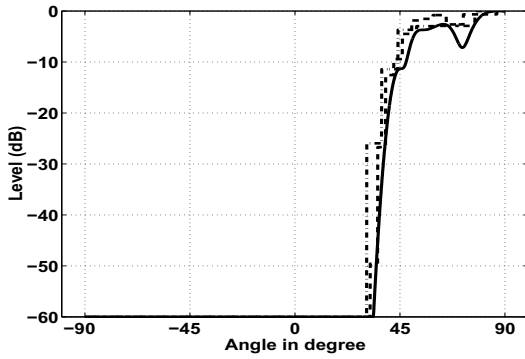


Figure 5: Ideal beampattern of $g(t)$ arriving at 90° on array 1 (solid line) and its digital beampattern using NN-interpolation with $f_s = 20$ GHz (dash-dotted line) and $f_s = 40$ GHz (dashed line)

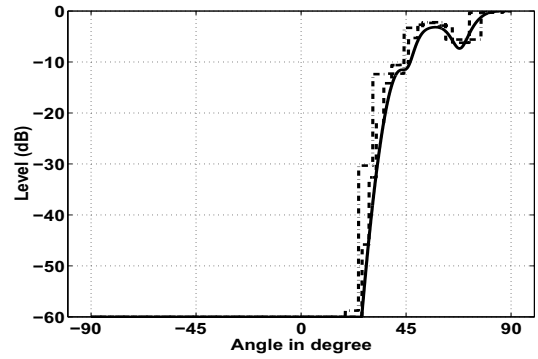


Figure 7: Ideal beampattern of $g_\alpha(t)$ arriving at 90° on array 1 (solid line) and its digital beampattern using NN-interpolation with $f_s = 20$ GHz (dash-dotted line) and $f_s = 40$ GHz (dashed line)

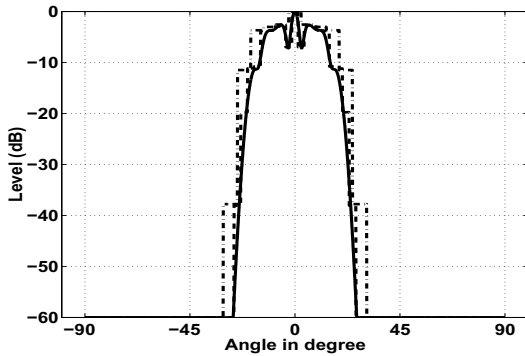


Figure 6: Ideal beampattern of $g(t)$ arriving at 0° on array 1 (solid line) and its digital beampattern using NN-interpolation with $f_s = 20$ GHz (dash-dotted line) and $f_s = 40$ GHz (dashed line)

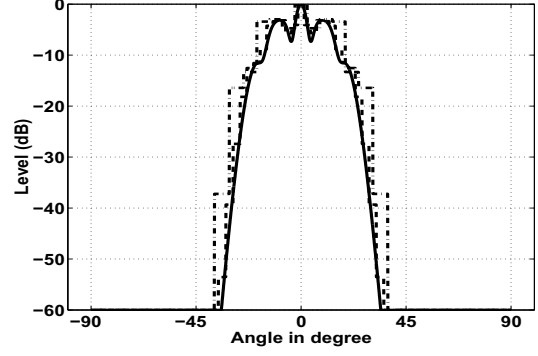


Figure 8: Ideal beampattern of $g_\alpha(t)$ arriving at 0° on array 1 (solid line) and its digital beampattern using NN-interpolation with $f_s = 20$ GHz (dash-dotted line) and $f_s = 40$ GHz (dashed line)

duce large errors. This detrimental effect can be reduced by heavily oversampling of the input signals [7]; however, due to the immense bandwidth of UWB signals, this seems to be unrealistic even within the next years. A better method is to use linear interpolation between the two nearest sampling points, which requires two multiplications for each desired signal value. This approach still produces large errors in the narrowband case without adequate oversampling [8]. It should be mentioned that these two interpolation methods are the optimum methods for the case that only one or two signal samples can be used to approximate a time-shifted signal value [1]. A theoretical treatment of the narrowband digital beampattern for various interpolation methods can be found in [9]; an extension to the broadband case is a topic of further research.

In Figures 5-12, the digital beampatterns for the 2 UWB pulses considered is compared to the ideal analog beampattern. The simulations are restricted to the case of array 1. In Figures 5-8, nearest-neighbour interpolation is used in order to approximate the true time delays at sampling frequencies $f_s = 20$ GHz and $f_s = 40$ GHz. In Figures 9-12, linear interpolation is used at sampling

frequencies $f_s = 20$ GHz and $f_s = 40$ GHz.

The use of broadband signals turns out to reduce the errors significantly in comparison to the narrowband case, and the digital beampattern of the UWB pulses are quite close to the ideal pattern, at least in the case of $f_s = 40$ GHz. This is due to the fact that in the narrowband case, the interpolation errors from different sensor signals can add constructively, while in the broadband case, the averaging effect reduces the interpolation errors. In fact, at $f_s = 40$ GHz, the cheapest method, namely nearest-neighbour interpolation which needs no multiplications, leads to an acceptable beampattern. This means that fortunately, digital delay-and-sum beamforming of UWB signals is not complicated from the viewpoint of pure digital signal processing complexity.

4. CONCLUSION

State-of-the-art in analog-digital-conversion are sampling frequencies up to 50 GHz, so that digital beamforming of UWB signals can be carried out in principal even nowadays. Nevertheless, such an approach is far away from its partial use for mobile devices and even

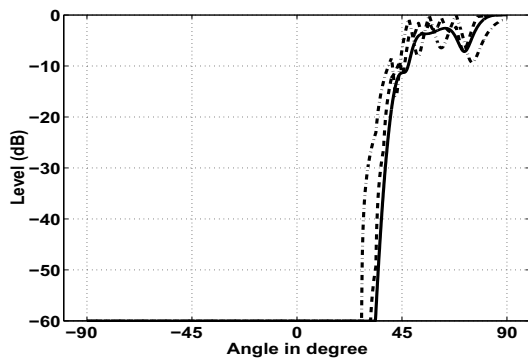


Figure 9: Ideal beampattern of $g(t)$ arriving at 90° on array 1 (solid line) and its digital beampattern using linear interpolation with $f_s = 20$ GHz (dash-dotted line) and $f_s = 40$ GHz (dashed line)

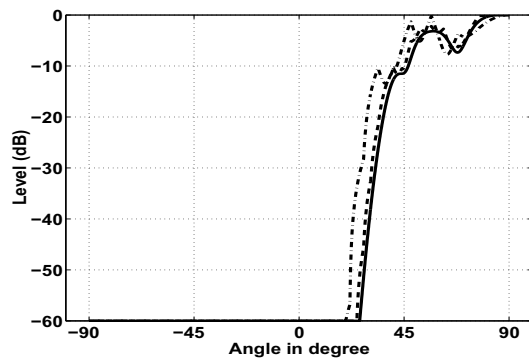


Figure 11: Ideal beampattern of $g_\alpha(t)$ arriving at 90° on array 1 (solid line) and its digital beampattern using linear interpolation with $f_s = 20$ GHz (dash-dotted line) and $f_s = 40$ GHz (dashed line)

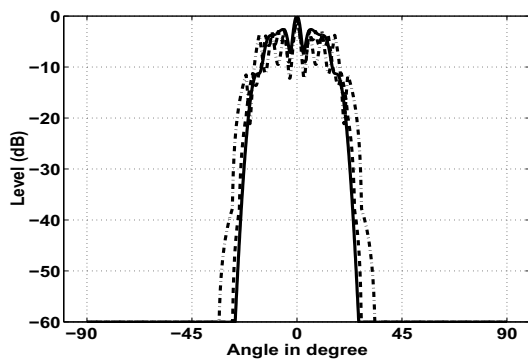


Figure 10: Ideal beampattern of $g(t)$ arriving at 0° on array 1 (solid line) and its digital beampattern using linear interpolation with $f_s = 20$ GHz (dash-dotted line) and $f_s = 40$ GHz (dashed line)

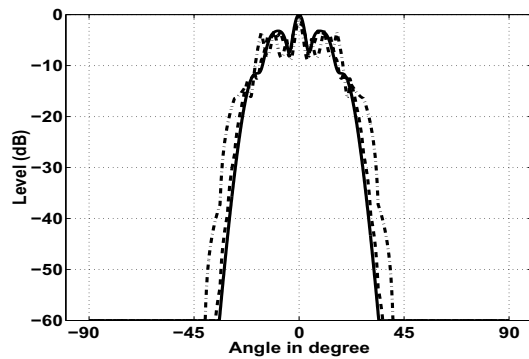


Figure 12: Ideal beampattern of $g_\alpha(t)$ arriving at 0° on array 1 (solid line) and its digital beampattern using linear interpolation with $f_s = 20$ GHz (dash-dotted line) and $f_s = 40$ GHz (dashed line)

for fixed access points because of their power consumption and immense hardware costs. However, according to Moore's law, technology will progress and with additional research in this area even digital beamforming of UWB communication signals may find its way in the future. This conjecture is further substantiated by recent results in related areas, e.g. breast cancer detection by UWB signals [2], where similar high-sampling digital beamformers are already realized and in use.

REFERENCES

- [1] T. Blu, P. Thevenaz, and M. Unser, "MOMS: Maximal-Order Interpolation of Minimal Support," *IEEE Transactions on Image Processing*, vol. 10, no. 7, 2001.
- [2] E. J. Bond, X. Li, S. C. Hagness, and B. v. d. Veen, "Microwave Imaging via Space-Time Beamforming for Early Detection of Breast Cancer," *IEEE Transactions on Antennas and Propagation*, vol. 51, no. 8, August 2003.
- [3] M. G. Hussain, "Principles of Space-Time Array Processing for Ultrawide-Band Impulse Radar and Radio Communications," *IEEE Trans. on Vehicular Technologies*, vol. 51, no. 3, 2002.
- [4] T. Kaiser, "UWB-Beamforming," in *Kleinheubacher Tagung, Session on Efficient Communication Systems using Smart Antennas*, September 2003, Kleinheubach, Germany.
- [5] T. Kaiser, "On the Usefulness of Multiple (Smart) Antennas for Ultra-Wideband Communications," IST Summit, June 2003, Aveiro, Portugal.
- [6] V. Murino, A. Trucco, and A. Tesei, "Beam Pattern Formulation and Analysis for Wide-band Beamforming Systems using Sparse Arrays," *Signal Processing*, vol. 56, 1997.
- [7] R. G. Pridham, and R. A. Mucchi, "Digital Interpolation Beamforming for Lowpass and Bandpass Signals," *Proc. IEEE*, vol. 67, no. 6, 1979.
- [8] D. Rathjen, G. Bödecker and M. Siegel, "Omnidirectional Beamforming for Linear Antennas by means of Interpolated Signals," *IEEE J. Oceanic Engineering*, vol. 10, no. 3, 1985.
- [9] S. Ries, "Digital Time-Delay Beamforming with Interpolated Signals," in *Proc. of the European Conference on Underwater Acoustics*, Elsevier Appl. Science, 1992.